

Predictor-Free and Hardware-Aware Federated Neural Architecture Search via Pareto-Guided Supernet Training

Bostan Khan
Mälardalen University
 Västerås, Sweden
 bostan.khan@mdu.se

Masoud Daneshatalab
Mälardalen University
 Västerås, Sweden
 masoud.daneshatalab@mdu.se

Abstract—Federated Neural Architecture Search (FedNAS) aims to automate model design for privacy-preserving Federated Learning (FL) but currently faces two critical bottlenecks: unguided supernet training that yields suboptimal models, and costly multi-hour pipelines for post-training subnet discovery. We introduce DeepFedNAS, a novel, two-phase framework underpinned by a multi-objective fitness function that synthesizes mathematical network design with architectural heuristics. Enabled by a re-engineered supernet, DeepFedNAS introduces *Federated Pareto Optimal Supernet Training*, which leverages a pre-computed Pareto-optimal cache of high-fitness architectures as an intelligent curriculum to optimize shared supernet weights. Subsequently, its *Predictor-Free Search Method* eliminates the need for costly accuracy surrogates by utilizing this fitness function as a direct, zero-cost proxy for accuracy, enabling on-demand subnet discovery in mere seconds. DeepFedNAS achieves state-of-the-art accuracy (e.g., up to 1.21% absolute improvement on CIFAR-100), superior parameter and communication efficiency, and a substantial $\sim 61\times$ speedup in total post-training search pipeline time. By reducing the pipeline from over 20 hours to approximately 20 minutes (including initial cache generation) and enabling 20-second individual subnet searches, DeepFedNAS makes hardware-aware FL deployments instantaneous and practical. The complete source code and experimental scripts are available at: <https://github.com/bostankhan6/DeepFedNAS>

Index Terms—Federated Learning, Neural Architecture Search, Supernet, Weight Sharing, Network Design, Efficiency

I. INTRODUCTION

The demand for intelligent, on-device applications, such as mobile keyboard prediction [2] and personalized

The computations in this work were enabled by resources provided by the National Academic Infrastructure for Supercomputing in Sweden (NAISS), partially funded by the Swedish Research Council through grant agreement no. 2022-06725.

A preliminary version of this work has been accepted at the ESANN 2026 conference [1]. This manuscript significantly extends the conference version with new theoretical analysis, a hardware-aware optimization framework, additional experiments, and deeper discussion.

healthcare [3], has driven the need for machine learning paradigms that are simultaneously computationally efficient and privacy-preserving. Federated Learning (FL) [4] has become the dominant paradigm to address this, facilitating collaborative model training on decentralized user data without exposing it. While FL provides a robust solution for *how* to train a given model, the challenge of determining *what* model architecture to train remains a significant bottleneck. This architectural design, often performed manually, is frequently suboptimal given the vast heterogeneity of data distributions and hardware capabilities across client devices [5].

To automate this critical design step, the research community has developed Federated Neural Architecture Search (FedNAS) to discover optimal network architectures directly within the federated setting [6]. Among the various FedNAS techniques, supernet-based methods have become the state-of-the-art due to their high cost efficiency, building on the success of centralized approaches like the Once-For-All (OFA) network [7]. The SuperFedNAS framework [8], in particular, marked a key advancement by decoupling the costly supernet training phase from a fast, training-free search phase. This innovation effectively reduced the training complexity of finding specialized subnets for multiple hardware targets from $O(N)$ to $O(1)$.

Despite this progress, the SuperFedNAS framework presents two fundamental challenges that limit its ultimate performance and practicality. First, the *training of the supernet itself is unguided and inefficient*. The baseline framework predominantly relies on random sampling of subnets (e.g., the Sandwich Rule’s uniform sampling component [9]) to update the shared weights. This unguided approach frequently selects suboptimal architectures, whose subsequent training provides noisy and conflicting gradient updates that can degrade the supernet’s shared weights and hinder the performance of higher-performing subnets. Second, the *post-training*

search for optimal subnets remains an energy-intensive, multi-stage pipeline. The standard methodology involves generating a large dataset of architecture-accuracy pairs by exhaustive subnet evaluation to train a separate accuracy predictor. This predictor pipeline acts as a prohibitive barrier to rapid experimentation and deployment, especially when tailoring models to new hardware constraints.

In this paper, we introduce **DeepFedNAS** (illustrated in Fig. 1), a novel, two-phase framework that comprehensively addresses these limitations to significantly advance federated supernet training and search. Our work is grounded in the observation that a mathematically motivated approach to architecture evaluation can fundamentally transform both the supernet training process and the subsequent search for optimal subnets. Inspired by the mathematical design concepts of DeepMAD [10], we construct a unified multi-objective fitness function, $\mathcal{F}(\mathcal{A})$, that synthesizes network information theory with empirical architectural heuristics. Crucially, we operationalize structural guidelines (like depth uniformity and channel monotonicity) as penalty terms, thereby enabling a holistic, single-objective optimization for all desired architectural properties within a federated, weight-sharing context. This unified fitness function underpins our two primary contributions.

First, to address the supernet training inefficiency, we propose *Federated Pareto Optimal Supernet Training*. Leveraging our fitness function, we perform an extensive, independent search to generate a pre-computed cache of Pareto-optimal architectures, which we term the “Pareto path”. This path serves as a Pareto-Guided training curriculum. Instead of random sampling, our methodology ensures the supernet’s shared weights are consistently updated by gradients from theoretically grounded, high-fitness architectures, thereby producing a superior final supernet. Additionally, to fully enable this guided search and overcome inherent limitations of prior supernet implementations, we introduce a *re-engineered, generic ResNet-based [11] supernet framework* that significantly expands the architectural search space and improves model fitness.

Second, we leverage the properties of our optimal path-guided trained supernet to introduce a *Predictor-Free Search Method*¹. After our supernet is trained using the path-guided curriculum, its shared weights are exceptionally well-conditioned for promising architectural patterns. We demonstrate that our mathematical fitness function, $\mathcal{F}(\mathcal{A})$, now serves as a high-fidelity, zero-cost proxy for the final accuracy of an extracted

¹In this work, the term ‘Predictor-Free’ specifically denotes the elimination of computationally expensive accuracy surrogates. However, we do utilize negligible-cost latency predictors for hardware constraints, as detailed in Section III-G2.

subnet. Consequently, we can find optimal architectures for any new deployment budget or hardware constraint by running a fast, on-demand genetic algorithm that maximizes this fitness function directly. This completely obviates the need for the costly, data-driven predictor pipeline used in prior work.

Our comprehensive DeepFedNAS framework not only achieves state-of-the-art accuracy across diverse datasets and non-IID conditions but also dramatically accelerates the post-training search. We demonstrate a $61\times$ speedup compared to the baseline, replacing a multi-hour predictor pipeline with a near-instantaneous search for specialized subnets adaptable to explicit hardware constraints like parameters and real-world latency.

In summary, our main contributions are:

- A unified, multi-objective fitness function for CNN-based subnets, which adapts and extends mathematical network design concepts [10] to formulate a single optimization problem for balancing network expressiveness with architectural stability and structural soundness within a federated, weight-sharing context.
- A *re-engineered, generic ResNet-based supernet framework* offering unparalleled flexibility in design and a significantly expanded architectural search space, crucial for enabling guided optimization and overcoming limitations of prior fixed supernet design [8].
- A *Federated Pareto Optimal Supernet Training* methodology, which leverages a pre-computed cache of elite, high-fitness architectures (the “Pareto path”) to serve as an effective and intelligent training curriculum, leading to a superior final supernet.
- A *Predictor-Free Search Method* that utilizes our multi-objective fitness function as a direct, zero-cost proxy for model performance, eliminating the entire costly predictor-training pipeline and dramatically reducing search costs by $\sim 61\times$.
- The end-to-end **DeepFedNAS** framework, which is validated through extensive experiments to show superior performance over state-of-the-art baseline methods, particularly in highly heterogeneous non-IID environments, and its capability to effectively optimize for diverse hardware constraints.

II. RELATED WORK

Our research is situated at the intersection of FL, Neural Architecture Search (NAS), and theory-driven network design. This section reviews the foundational concepts and key advancements in these areas, thereby contextualizing our proposed methodology which builds upon recent progress in cost-efficient federated architecture search.

A. Federated Learning

FL has emerged as the dominant paradigm for distributed machine learning that preserves data privacy [12], enabling applications ranging from mobile keyboard prediction [2] to sensitive healthcare analytics [3]. In the standard FL setting, a central server coordinates the training of a global model across decentralized clients without requiring access to raw data [4]. The seminal algorithm, Federated Averaging (FedAvg) [4], involves clients training locally and transmitting only model updates for aggregation. This paradigm has spurred a vast field of research, with open challenges and advances cataloged in several comprehensive surveys [13]–[15].

A primary challenge in FL is statistical heterogeneity, where client data is not independent and identically distributed (non-IID) [16]. This non-IID nature—comprehensively reviewed in [17]—can significantly degrade model performance and slow convergence. A second, equally critical challenge is *system heterogeneity*, where clients possess diverse hardware with varying computational, memory, and energy resources [5]. These challenges motivate the need for methods that can produce personalized FL models tailored to individual client data distributions [18], [19] and hardware capabilities [20].

B. Neural Architecture Search with Weight Sharing

While FL addresses how to train a model, NAS tackles the challenge of designing the model architecture itself. Early NAS methods, often based on reinforcement learning [21] or evolutionary algorithms [22], were computationally prohibitive. The introduction of weight-sharing via a supernet [23], [24], particularly through differentiable approaches like DARTS [25], dramatically improved efficiency.

The OFA network [7] serves as a cornerstone of this paradigm. OFA trains a single, large supernet containing a vast number of sub-architectures. By using a progressive shrinking training schedule, OFA ensures subnets can be extracted to meet diverse hardware constraints without costly retraining. Similarly, BigNAS [26] popularized the “Sandwich Rule” sampling strategy [9] to simultaneously optimize the largest, smallest, and random subnets.

However, the weight-sharing paradigm is not without flaws. Naively sharing weights can lead to poor rank correlation between supernet estimation and true standalone accuracy [27]. This is often attributed to interference or multi-model forgetting, where training one subnet degrades the performance of others sharing the same weights [28], [29]. While recent centralized works have explored advanced strategies to mitigate this [30], [31], adapting such concepts to the constrained

federated setting remains an open challenge and the key focus of our work.

C. Federated Neural Architecture Search

FedNAS combines FL and NAS to automate architecture design in a federated setting. Early works like FedNAS [6] and [32] demonstrated the feasibility of this concept.

The central challenge for FedNAS is the confluence of statistical (non-IID) and system (hardware) heterogeneity [33]. A “one-size-fits-all” architecture is often suboptimal, leading to two main branches of research:

- 1) **Data Personalization:** Many works focus on adapting the architecture to local data. For instance, [34] allows clients to find a locally optimal path through a global supernet for 3D medical segmentation. Other methods, such as Peaches [35] and FedPNAS [36], use a “base-and-personal” structure, while others employ reinforcement learning [37], [38] or knowledge distillation [39], [40] to manage heterogeneity.
- 2) **System Efficiency (Our Focus):** Other approaches leverage the supernet paradigm to handle *system* heterogeneity. The goal is to create a single global supernet from which clients can extract subnets of different sizes [41]. However, many such methods suffer from two limitations highlighted by [8]:
(1) prohibitive computational costs due to tightly coupled search and training phases [42], [43]; and
(2) restricted search spaces that limit diversity [44].

Our research builds upon the SuperFedNAS framework [8], which addressed the cost limitation by decoupling supernet training from the search phase. While efficient ($O(1)$ search cost), we identify that SuperFedNAS relies on unguided random sampling (e.g., Sandwich Rule), leading to inefficient weight updates. Our approach resonates with recent advances in *centralized* NAS that critique random sampling: DC-NAS [30] proposes diversified sampling to balance exploration, while PreNAS [31] utilizes a zero-cost proxy to focus training on high-quality candidates. We are the first to adapt these advanced sampling concepts to the challenging federated environment.

D. Mathematical Frameworks for Architecture Design

The majority of NAS methods, including OFA [7] and SuperFedNAS [8], rely on heuristic-driven search algorithms that treat the network as a black box whether based on gradient descent [25], evolution [45], or even priors from Large Language Models [46], [47]. An alternative and emerging direction is to design networks based on intrinsic mathematical properties.

The DeepMAD framework [10] is a prominent example, proposing a mathematical method for designing efficient CNNs by maximizing metrics representing

network information entropy and effectiveness. Other information-theoretic approaches utilize mutual information analysis to guide search by pruning less contributory layers [48].

Our work is the first to adapt and extend these mathematical concepts for the fundamentally different problem of federated supernet training. We do not use DeepMAD as a one-shot architecture generator; instead, we synthesize its core concepts with empirical heuristics to create a multi-objective fitness function tailored for evaluating subnets within a weight-sharing paradigm. This unified formulation unlocks our two main contributions: *Federated Pareto Optimal Supernet Training*, which uses a pre-computed curriculum of elite architectures, and a *Predictor-Free Search Method*, which leverages the fitness function as a direct, zero-cost proxy for performance.

III. METHODOLOGY

Our work introduces DeepFedNAS, a unified, two-phase framework that significantly advances federated supernet design and search. Central to our methodology is a multi-objective fitness function (Section III-C), which synthesizes and adapts the information-theoretic concepts of DeepMAD into a unified searchable metric for the unique constraints of federated, weight-sharing architectures. This function underpins our contributions: first, enabling an independent search (Section III-D) to generate a Pareto-optimal path of elite architectures; second, driving our Federated Pareto Optimal Supernet Training (Section III-E), which leverages this path as a Pareto-guided curriculum; and finally, facilitating a highly efficient Predictor-Free Search Method (Section III-F) that directly optimizes against our fitness function. Furthermore, to overcome architectural limitations of prior work, we develop a re-engineered, generic supernet framework (Section III-B) enabling flexibility and improved architectural fitness. This comprehensive approach ensures a superior final supernet and an extremely efficient search mechanism, capable of hardware-aware deployment optimization (Section III-G). The overall DeepFedNAS pipeline, illustrating the main interconnected phases, is depicted in Fig. 1. We begin by formulating the federated supernet training problem and highlighting the limitations of existing random sampling approaches.

A. Problem Formulation: Federated Supernet Training

The objective of federated supernet training is to learn a single set of shared weights, W , that can effectively serve a vast architectural search space, \mathbb{S} , across K decentralized clients. Each client k possesses a unique local data partition \mathcal{D}_k . The overarching goal is to find a set of weights W that minimizes the expected loss

over all possible architectures $\mathcal{A} \in \mathbb{S}$ and all client data distributions:

$$\min_W \mathbb{E}_{\mathcal{A} \in \mathbb{S}} \left[\sum_{k=1}^K \frac{|\mathcal{D}_k|}{|\mathcal{D}|} \mathcal{L}_k(\mathcal{G}(W, \mathcal{A})) \right] \quad (1)$$

where $\mathcal{G}(W, \mathcal{A})$ denotes the function that extracts a specific subnet's weights from the shared supernet W , and \mathcal{L}_k is the loss on client k 's local data.

The training process involves the following multi-step procedure in each round t :

- 1) A subset of available clients, \mathcal{K}_t , is selected.
- 2) For each client $k \in \mathcal{K}_t$, a subnet architecture $\mathcal{A}_k \in \mathbb{S}$ is assigned. The corresponding weights $w_{k,t} = \mathcal{G}(W_t, \mathcal{A}_k)$ are extracted and sent.
- 3) Each client trains $w_{k,t}$ on \mathcal{D}_k , producing updated weights $w'_{k,t}$.
- 4) The server receives updates and performs an overlap-aware aggregation to update W_{t+1} .

The **SuperFedNAS framework** [8] serves as our baseline, specifically for its aggregation mechanism. To handle the sparse updates inherent in supernet training (Step 4), we employ **MaxNet** with an overlap-aware scaling factor. We refine the formalization of this aggregation using precise binary mask notation to account for parameter overlap. Let $\mathbb{I}_k(\theta) \in \{0, 1\}$ indicate if a specific parameter θ is active in the architecture \mathcal{A}_k assigned to client k . The server update Δ_θ at round t is computed as:

$$\Delta_\theta = \frac{\beta_t \mathbb{I}_{\max}(\theta) \Delta_{k_{\max}}(\theta) + (1 - \beta_t) \sum_{k \in \mathcal{K}'} \mathbb{I}_k(\theta) \Delta_k(\theta)}{\beta_t \mathbb{I}_{\max}(\theta) + (1 - \beta_t) \sum_{k \in \mathcal{K}'} \mathbb{I}_k(\theta) + \epsilon} \quad (2)$$

where $\mathcal{K}' = \mathcal{K}_t \setminus \{k_{\max}\}$ denotes the set of clients excluding the one training the largest subnet. The term ϵ is a small constant added for numerical stability. Here, $\Delta_k(\theta) = w'_{k,t}(\theta) - W_t(\theta)$ is the local update, k_{\max} is the client assigned the largest subnet (\mathcal{A}_{\max}), and $\beta_t \in [0, 1]$ is a dynamic weighting coefficient that anneals over time using cosine scheduling. This aggregation ensures that shared weights are updated proportionally to their usage frequency. The global model is then updated as $W_{t+1}(\theta) = W_t(\theta) + \eta_g \cdot \Delta_\theta$.

The critical challenge lies in the sampling strategy (Step 2). SuperFedNAS's random sampling component is unguided. The architectural search space \mathbb{S} is not only vast but also qualitatively uneven; the overwhelming majority of possible architectures are mediocre. This leads to inefficient gradient updates and a limited training curriculum. This fundamental limitation motivates our work.

B. Supernet Framework and Search Space Definition

Our initial investigation revealed that the baseline SuperFedNAS search space was inherently constrained,

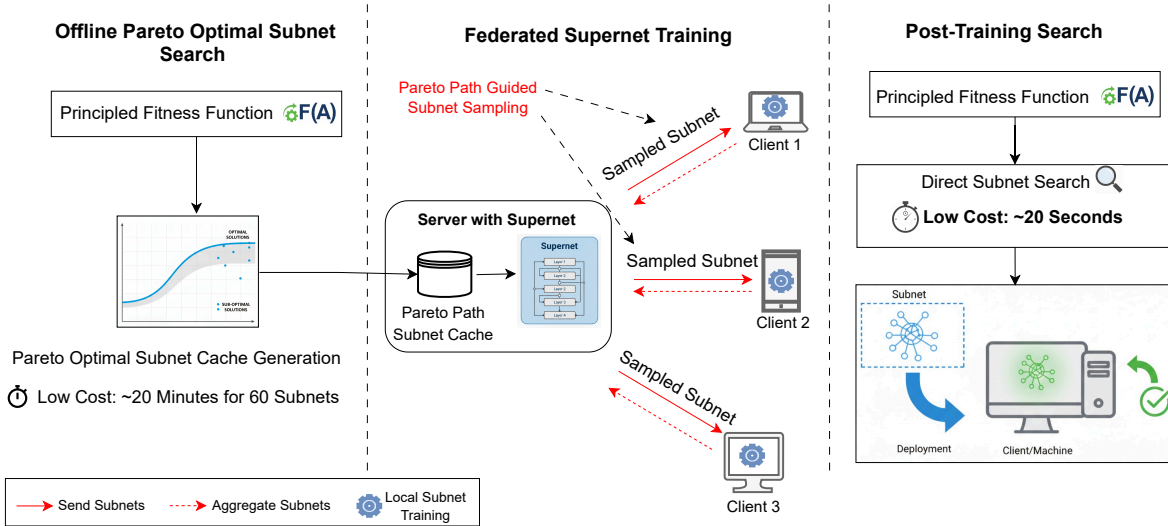


Fig. 1: DeepFedNAS Pipeline. This diagram illustrates the three core phases of our framework. First, the **Offline Pareto Optimal Subnet Search** generates a “Pareto Path Subnet Cache” of high-fitness architectures (e.g., 60 subnets in ~ 20 minutes) using a multi-objective fitness function $\mathcal{F}(\mathcal{A})$. Second, the **Federated Supernet Training** leverages this cache for “Pareto Path Guided Subnet Sampling,” where clients are assigned highly effective architectures for local training, improving supernet weight quality. Finally, the **Post-Training Search** directly optimizes against $\mathcal{F}(\mathcal{A})$ to find an optimal subnet for deployment (e.g., in ~ 20 seconds), completely bypassing the need for a costly predictor pipeline.

yielding architectures with consistently low fitness scores (Section III-C), as clearly illustrated by the limitations of the baseline’s constrained search space and unguided random sampling shown in Fig. 2. This motivated a re-engineered, generic ResNet-based supernet framework. This new framework is highly configurable, supporting a variable number of stages (S) and fine-grained control over architectural choices within each stage.

We formally define the search space \mathbb{S} . For a supernet with S stages, we define three distinct sets of discrete choices:

- $D = \{d_1, \dots, d_K\}$: The set of choices for the number of blocks (depth) in a stage.
- $C = \{c_1, \dots, c_M\}$: The set of choices for channel width multipliers.
- $E = \{e_1, \dots, e_P\}$: The set of choices for bottleneck expansion ratios.

An architecture $\mathcal{A} \in \mathbb{S}$ is uniquely represented by a genome consisting of three concatenated vectors:

$$\mathcal{A} = (\mathbf{d}, \mathbf{e}, \mathbf{w}) \quad (3)$$

where:

- $\mathbf{d} \in D^S$: A depth vector of length S , where d_i is the number of extra blocks in stage i .
- $\mathbf{e} \in E^{S \times N_{\text{blocks}}}$: An expansion ratio vector. To allow for a fixed-length genome despite variable depth,

we assign an expansion gene to every possible block slot in the supernet (total $S \times N_{\text{blocks}}$ slots), even if inactive.

- $\mathbf{w} \in C^{S+1}$: A width vector of length $S + 1$, specifying the multiplier for the stem (w_0) and each stage (w_1, \dots, w_S).

The full search space \mathbb{S} is the Cartesian product of these vector spaces:

$$\mathbb{S} = D^S \times E^{S \times N_{\text{blocks}}} \times C^{S+1} \quad (4)$$

This formal definition accurately reflects our implementation, where the genome is a flat vector concatenating depth, expansion, and width decisions. As demonstrated in our experimental setup (see Table I), this design enables a significantly broader range of model complexities compared to the baseline.

C. An Entropy-Based, Multi-Objective Fitness Function

To overcome random sampling, we require a mechanism to evaluate an architecture’s quality without costly training. We develop a multi-objective fitness function, $\mathcal{F}(\mathcal{A})$, inspired by the mathematical design framework of DeepMAD [10], which balances network expressiveness (entropy) against architectural stability (effectiveness). We synthesize these concepts with structural guidelines (depth uniformity, channel monotonicity), reformulating them as penalty terms.

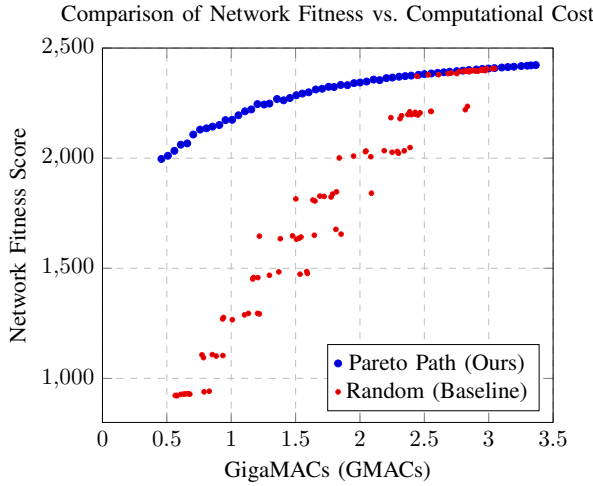


Fig. 2: Comparison of architectures discovered by our multi-objective search (Pareto Path) versus a uniform random sampling baseline. Our search method consistently discovers a Pareto-optimal frontier of architectures with significantly higher network fitness scores for any given computational budget (GigaMACs). This pre-computed cache of elite subnets forms the basis of our path-guided training, avoiding the suboptimal, low-fitness architectures frequently chosen by the baseline’s random sampler.

Our unified fitness function for an architecture $\mathcal{A} \in \mathbb{S}$ is:

$$\begin{aligned} \mathcal{F}(\mathcal{A}) = \sum_{j=1}^S \alpha_j H_j(\mathcal{A}) - \omega Q(\mathcal{A}) + \lambda \rho(\mathcal{A}) - \gamma V(\mathcal{A}) \\ \text{s.t. } \rho(\mathcal{A}) \leq \rho_0 \end{aligned} \quad (5)$$

where $\alpha_j, \omega, \lambda, \gamma$ are weighting hyper-parameters. Given the architecture genome $\mathcal{A} = (\mathbf{d}, \mathbf{e}, \mathbf{w})$, the components are defined as follows:

- **Stage-wise Network Entropy** ($H_j(\mathcal{A})$): A proxy for the expressive power of stage j . Let r_j be the feature map resolution at stage j ’s end, and $c_{\text{out},j}$ be the output width. Let $c_{\text{in},\ell}(\mathcal{A})$ be the input width of layer ℓ (determined by \mathbf{w} and \mathbf{e}), and k_ℓ be its kernel size. The entropy for stage j sums the contributions of its active layers:

$$H_j(\mathcal{A}) = \log(r_j^2 \cdot c_{\text{out},j}) \sum_{\ell \in \text{Stage}_j} \log(c_{\text{in},\ell} \cdot k_\ell^2) \quad (6)$$

Here, the inner summation iterates only over the active layers ℓ configured by the depth vector \mathbf{d} for stage j .

- **Effectiveness** ($\rho(\mathcal{A})$): A measure of architectural stability. Let $L(\mathcal{A})$ be the total depth of active layers.

$$\rho(\mathcal{A}) = \frac{L(\mathcal{A})}{\exp\left(\frac{1}{L(\mathcal{A})} \sum_{\ell \in \text{Active}} \log(c_{\text{in},\ell}(\mathcal{A}) \cdot k_\ell^2)\right)} \quad (7)$$

- **Depth Uniformity Penalty** ($Q(\mathcal{A})$): A penalty for non-uniform stage depths, captured by the variance of the stage depth vector \mathbf{d} .

$$Q(\mathcal{A}) = \exp(\text{Var}(\mathbf{d})) \quad (8)$$

- **Channel Monotonicity Penalty** ($V(\mathcal{A})$): A penalty for violating non-decreasing channel counts. Let $w_{\text{out},i}(\mathcal{A})$ be the output channel count of stage i derived from \mathbf{w} .

$$V(\mathcal{A}) = \sum_{i=0}^{S-1} \max(0, w_{\text{out},i}(\mathcal{A}) - w_{\text{out},i+1}(\mathcal{A})) \quad (9)$$

This unified function is maximized during our offline search, subject to hard constraints $\text{MACs}(\mathcal{A}) \leq \text{Budget}$ and $\rho(\mathcal{A}) \leq \rho_0$.

D. Search for Optimal Path Generation

We perform an extensive, offline search to generate a cache of elite subnets, \mathcal{C} , termed the “optimal path cache.” We discretize the computational range into N target budgets, $\mathcal{B} = \{B_1, \dots, B_N\}$. We then solve N independent optimization problems to find, for each budget $B_i \in \mathcal{B}$, the optimal architecture \mathcal{A}_i^* :

$$\mathcal{A}_i^* = \arg \max_{\mathcal{A} \in \mathbb{S}} \mathcal{F}(\mathcal{A}) \quad \text{subject to} \quad \text{MACs}(\mathcal{A}) \leq B_i \quad (10)$$

Each optimization (Eq. 10) is solved using a dedicated instance of a standard genetic algorithm. To ensure efficiency and validity, we employ a **rejection sampling initialization**: we randomly generate architectures and immediately discard any that violate the MACs or ρ_0 constraints, repeating until the initial population $P^{(0)}$ consists entirely of valid candidates.

The GA proceeds as follows:

- 1) **Selection:** Tournament selection is used to choose parents from the current population $P^{(g)}$.
- 2) **Crossover:** Single-point crossover combines the genomes $\mathcal{A}_a, \mathcal{A}_b$ to produce offspring.
- 3) **Mutation:** With probability p_m , genes in \mathbf{d} , \mathbf{e} , or \mathbf{w} are randomly reset to new valid values from their respective choice sets.
- 4) **Elitism:** The best architecture found so far is preserved across generations.

The final aggregated set of elite architectures, $\mathcal{C} = \{\mathcal{A}_1^*, \dots, \mathcal{A}_N^*\}$, forms a robust approximation of the true Pareto-optimal frontier. The size of this cache, N , is a hyperparameter chosen to ensure sufficient granularity

Algorithm 1 DeepFedNAS: Federated Pareto Optimal Supernet Training

Require: Supernet weights W_0 , Pareto Cache \mathcal{C} , Clients K , Rounds T , Clients per round C , Learning rate η .
Ensure: Optimized Supernet Weights W_T .

- 1: **Server:** Generate Pareto Path Cache \mathcal{C} (Section III-D).
- 2: **for** $t = 0$ to $T - 1$ **do**
- 3: **Server:** Select subset of clients \mathcal{K}_t (size $C \cdot K$).
- 4: **for** each client $k \in \mathcal{K}_t$ **do**
- 5: **Server:** Determine architecture assignment \mathcal{A}_k using Pareto Path Sampling:

$$\mathcal{A}_k \leftarrow S(k, \mathcal{C}) \quad (\text{Eq. 11})$$
- 6: **Server:** Send active weights $w_{k,t} = \mathcal{G}(W_t, \mathcal{A}_k)$ to client k .
- 7: **Client k :** Update weights locally on \mathcal{D}_k :

$$w'_{k,t} \leftarrow w_{k,t} - \eta \nabla \mathcal{L}_k(w_{k,t})$$
- 8: **Client k :** Compute update $\Delta_k = w'_{k,t} - W_t$ and upload.
- 9: **end for**
- 10: **Server:** Aggregation using Overlap-Aware MaxNet:
for each parameter θ in supernet **do**
- 11: Compute Δ_θ using binary masks $\mathbb{I}_k(\theta)$ (Eq. 2)
- 12: $W_{t+1}(\theta) \leftarrow W_t(\theta) + \eta_g \Delta_\theta$
- 13: **end for**
- 14: **end for**
- 15: **return** W_T

across the FL computational spectrum; in our experiments, we analyze the convergence properties of N to ensure statistical robustness (see Section IV-H1).

E. Federated Pareto Optimal Supernet Training

We formalize our training procedure in Algorithm 1. This training algorithm replaces the unguided random sampling of the baseline with a structured curriculum derived from the Pareto path cache \mathcal{C} . In each federated round t , the assignment of an architecture \mathcal{A}_k to a client k is governed by our Pareto Path assignment function $S(k, \mathcal{C})$:

$$\mathcal{A}_k = S(k, \mathcal{C}) = \begin{cases} \mathcal{A}_{\min} & \text{if } k \in \mathcal{K}_{t,\min} \\ \mathcal{A}_{\max} & \text{if } k \in \mathcal{K}_{t,\max} \\ \text{Uniform}(\mathcal{C}) & \text{otherwise} \end{cases} \quad (11)$$

where $\mathcal{A}_{\min}, \mathcal{A}_{\max} \in \mathcal{C}$ are the boundary architectures from our cache, and $\mathcal{K}_{t,\min}, \mathcal{K}_{t,\max}$ are the sets of clients who have trained these boundary architectures least frequently. This strategy ensures the supernet's weights are consistently updated based on gradients from a curriculum of optimized, high-entropy architectures.

F. Entropy-Based Fitness as a Predictor for Efficient Search

A major contribution of DeepFedNAS is a Predictor-Free Search Method, which circumvents the high computational cost of training and maintaining accuracy predictors (e.g., surrogate models). This capability stems directly from our unified multi-objective fitness formulation, $\mathcal{F}(\mathcal{A})$, and our Path-Guided Training strategy.

We posit that by constraining the supernet training to a curriculum of high-fitness architectures (via the Pareto Path Subnet Cache), we condition the shared weights W^* such that the structural fitness $\mathcal{F}(\mathcal{A})$ becomes a direct proxy for validation accuracy. While grounded in the information-theoretic concepts of entropy and effectiveness [10], our unified formulation transforms these theoretical bounds into a practical, searchable metric for federated supernets.

Formally, this relationship allows us to substitute the expensive expectation of accuracy with our zero-cost fitness function:

$$\arg \max_{\mathcal{A} \in \mathcal{S}} \mathbb{E}[\text{Acc}(\mathcal{A}, W^*)] \approx \arg \max_{\mathcal{A} \in \mathcal{S}} \mathcal{F}(\mathcal{A}) \quad (12)$$

Consequently, the deployment search for $\mathcal{A}_{\text{deploy}}^*$ becomes a swift, direct optimization of Eq. 5 using a genetic algorithm, completely obviating the need for a data-driven predictor pipeline. This allows the search to complete in seconds rather than hours. We provide empirical validation of the correlation between $\mathcal{F}(\mathcal{A})$ and true accuracy in Section IV-H3.

G. Additional Hardware Constraints for Deployment

Our framework supports hardware-aware deployment by integrating constraints such as parameters and latency into the final search.

1) *Integrating Model Parameters:* For memory-limited devices, we integrate an explicit upper bound on parameters (Params(\mathcal{A})) as a *hard constraint* during the deployment search:

$$\text{Params}(\mathcal{A}) \leq \text{ParamBudget}_M \quad (13)$$

2) *Integrating Inference Latency:* We employ a *Latency Predictor Model* (LPM) to estimate inference latency, denoted as $\mathcal{L}_{\text{pred}}(\mathcal{A}, \text{Device})$. It is crucial to distinguish the computational nature of this LPM from the accuracy predictors used in prior work. Accuracy predictors require the generation of a dataset containing (subnet architecture, accuracy) pairs. Constructing this dataset is prohibitively expensive because measuring the ground-truth accuracy of a single subnet necessitates a full inference pass over the entire validation set. Iterating this process for thousands of architectures to train a predictor creates a computational bottleneck.

In sharp contrast, training an LPM requires a dataset of (subnet architecture, latency) pairs. Measuring ground-truth latency is computationally inexpensive: it involves passing a single sample input (e.g., one image tensor) through the subnet on the target device to record the inference time. This process is deterministic and independent of the validation dataset size. Consequently, data collection for the LPM is orders of magnitude faster than for accuracy predictors. We define our approach as “Predictor-Free” in the specific sense that it eliminates the need for expensive accuracy surrogates, while utilizing lightweight, negligible-cost latency predictors to ensure hardware compliance.

The LPM is implemented as a lightweight MLP, $f_{\theta_{LPM}}$, trained offline. We formalize its components:

- 1) **Architecture Featurization:** An architecture $\mathcal{A} = (\mathbf{d}, \mathbf{e}, \mathbf{w})$ is transformed into a fixed-length vector $v_{\mathcal{A}}$ via concatenation of values from the depth, expansion, and width vectors:

$$v_{\mathcal{A}} = \text{Concat}(\text{feat}(\mathbf{d}), \text{feat}(\mathbf{e}), \text{feat}(\mathbf{w}), \text{MACs}(\mathcal{A}), \text{Params}(\mathcal{A})) \quad (14)$$

We explicitly include MACs and Parameters as features to enhance prediction accuracy.

- 2) **Model Definition:** The LPM maps the feature vector to a scalar latency: $\mathcal{L}_{\text{pred}}(\mathcal{A}, \text{Device}) = f_{\theta_{LPM}}(v_{\mathcal{A}})$.
- 3) **Training Objective:** The parameters θ_{LPM} are learned by minimizing the Mean Squared Error (MSE) on a measured dataset $\mathcal{D}_{\text{lat}} = \{(v_{\mathcal{A}_i}, \mathcal{L}_{\text{true},i})\}_{i=1}^M$ for a specific target Device:

$$\min_{\theta_{LPM}} \frac{1}{M} \sum_{i=1}^M (f_{\theta_{LPM}}(v_{\mathcal{A}_i}) - \mathcal{L}_{\text{true},i})^2 \quad (15)$$

This fast-to-train LPM allows latency to be incorporated into the deployment search as either a **hard constraint** ($\mathcal{L}_{\text{pred}}(\mathcal{A}, \text{Device}) \leq \text{LatencyBudget}_{\text{ms}}$) or as a **soft objective** by modifying the fitness function:

$$\mathcal{F}_{\text{deploy}}(\mathcal{A}) = \mathcal{F}(\mathcal{A}) - \delta \cdot \mathcal{L}_{\text{pred}}(\mathcal{A}, \text{Device}) \quad (16)$$

where $\delta > 0$ is a tunable penalty weight.

The final, hardware-aware deployment search for $\mathcal{A}_{\text{deploy}}^*$ is formulated as a comprehensive, multi-objective optimization:

$$\begin{aligned} \mathcal{A}_{\text{deploy}}^* = \arg \max_{\mathcal{A} \in \mathbb{S}} \mathcal{F}_{\text{deploy}}(\mathcal{A}) \\ \text{subject to } \text{MACs}(\mathcal{A}) \leq \text{Budget}_{\text{deploy}}, \\ \text{Params}(\mathcal{A}) \leq \text{ParamBudget}_{\text{M}}, \\ \mathcal{L}_{\text{pred}}(\mathcal{A}, \text{Device}) \leq \text{LatencyBudget}_{\text{ms}} \\ \text{(optional hard constraint)} \end{aligned} \quad (17)$$

where $\mathcal{F}_{\text{deploy}}(\mathcal{A})$ uses Eq. 16 if a soft latency objective is chosen, or Eq. 5 otherwise.

IV. EXPERIMENTS

We conduct a series of experiments to validate the effectiveness of the DeepFedNAS framework. Our evaluation is designed to answer four primary research questions:

- 1) **Does Pareto Optimal Supernet Training produce a superior supernet?** We compare the performance of subnets extracted from our DeepFedNAS-trained supernet against those from a supernet trained with other methods, specifically, the standard SuperFedNAS baseline.
- 2) **How effective is our Predictor-Free Search?** We evaluate the quality of architectures found by our on-demand fitness-driven search and quantify the reduction in computational cost compared to traditional predictor-based pipelines.
- 3) **How robust is our methodology?** We analyze the performance of our framework under varying FL conditions, including data heterogeneity and sparse client participation.
- 4) **Can DeepFedNAS effectively optimize for diverse hardware constraints?** We demonstrate the framework’s ability to discover high-performing subnets while adhering to explicit parameter and latency budgets.

We begin by detailing our experimental setup before presenting our main results and ablation studies.

A. Experimental Setup

a) **Datasets and Data Partitioning:** Our experiments are conducted on **CIFAR-10**, **CIFAR-100**, and **CINIC-10**. To ensure a fair and direct comparison, we replicate the exact data partitioning and federated setup described in the original SuperFedNAS paper [8]. Statistical heterogeneity is introduced by partitioning data among clients using a Dirichlet distribution [49]. For our main comparison, we use a concentration parameter of $\alpha = 100$ to maintain consistency with the baseline. We further evaluate robustness by varying this parameter to $\alpha = 1$ and $\alpha = 0.1$ in our heterogeneity analysis (Section IV-C). The partition settings are: $K = 20$ clients for **CIFAR-10** and **CIFAR-100**, and $K = 100$ clients for the larger **CINIC-10** dataset.

b) **Evaluation Protocol:** We adopt an evaluation protocol consistent with established resource-constrained federated NAS research [6], [8]. The training set is used

TABLE I: Supernet Search Space Comparison

Metric	SuperFedNAS	DeepFedNAS
Min. MACs (M)	458.97	7.55
Min. Params (M)	10.40	0.13
Max. MACs (M)	3,403.37	3,403.37
Max. Params (M)	71.73	71.73

TABLE II: Comparison on Image Datasets. We compare DeepFedNAS with baselines on CIFAR-10, CIFAR-100, and CINIC-10 for different MACs targets. DeepFedNAS consistently finds superior architectures, especially on more complex datasets like CIFAR-100.

Billion MACs	Method	Test Accuracy (%)		
		CIFAR-10	CIFAR-100	CINIC-10
0.45-0.95	FedAvg	85.25 \pm 0.46	43.19 \pm 0.54	61.76 \pm 0.78
	FedNAS	77.33 \pm 0.31	40.92 \pm 2.21	58.15 \pm 0.18
	FedPNAS	88.83 \pm 0.5	45.77 \pm 0.68	64.3 \pm 0.98
	SuperFedNAS	93.47 \pm 0.08	60.92 \pm 0.10	75.69 \pm 0.29
	DeepFedNAS (Ours)	94.16 \pm 0.18	62.60 \pm 0.16	77.04 \pm 0.39
0.95-1.45	FedAvg	86.36 \pm 0.22	43.92 \pm 0.57	63.00 \pm 0.17
	FedPNAS	89.27 \pm 0.81	47.8 \pm 2.6	65.74 \pm 0.32
	SuperFedNAS	93.52 \pm 0.16	61.66 \pm 0.37	76.53 \pm 0.19
	DeepFedNAS (Ours)	94.51 \pm 0.02	62.87 \pm 0.13	77.60 \pm 0.02
1.45-2.45	FedAvg	87.59 \pm 0.27	44.4 \pm 0.56	64.00 \pm 0.07
	FedNAS	86.41 \pm 0.1	45.82 \pm 0.29	59.97 \pm 0.27
	SuperFedNAS	93.72 \pm 0.01	62.06 \pm 0.06	77.09 \pm 0.07
	DeepFedNAS (Ours)	94.50 \pm 0.02	63.09 \pm 0.08	77.80 \pm 0.06
2.45-3.75	FedAvg	89.44 \pm 0.67	45.00 \pm 0.27	65.02 \pm 0.13
	FedNAS	89.43 \pm 0.36	58.39 \pm 0.23	71.93 \pm 0.13
	SuperFedNAS	93.72 \pm 0.02	62.30 \pm 0.01	77.09 \pm 0.07
	DeepFedNAS (Ours)	94.51 \pm 0.00	63.20 \pm 0.00	77.85 \pm 0.09

exclusively for local client model updates. The validation set serves a dual critical role: (1) monitoring progress to select the best supernet checkpoint, and (2) performing the final evaluation (accuracy, parameters, latency) of the subnets identified by the respective search algorithms. This strictly separated protocol ensures a consistent and computationally feasible comparison.

c) Supernet Architecture: To evaluate our method across a complex design space, we utilize the generic ResNet-style supernet framework detailed in Section III-B. For these experiments, we instantiate a 4-stage supernet with base channel sizes of [256, 512, 1024, 2048]. The search space is defined by three variable dimensions: depth $d \in \{1, 2, 3\}$ blocks per stage; width w with multipliers from 0.1 to 1.0 in steps of 0.1; and bottleneck expansion ratios $e \in \{0.1, 0.14, 0.18, 0.22, 0.25\}$. This results in a combinatorial space of approximately 1.98×10^{15} architectures, significantly larger than prior work (see Table I).

d) Search Space Exploration and Budget Alignment: Our re-engineered supernet is capable of representing architectures ranging from a mere 7.55 M MACs up to 3,403 M MACs. However, the SuperFedNAS baseline is structurally limited to a narrower range (458 M to 3,403 M MACs). To ensure a strictly fair comparison, we focus our architecture search and reporting within this shared performance-budget intersection. Specifically, our Pareto path cache (Section III-D) is generated starting from ≈ 458.2 M MACs. This alignment ensures that our performance gains are attributable to our proposed training methodology rather than simply expanding the search space into ultra-low resource regimes that the baseline cannot access.

e) Federated Training: We adhere to the baseline training parameters: a client participation rate of $C = 0.4, 5$ local epochs per round, and an SGD optimizer with cosine decay. Notably, during replication, we observed that increasing gradient clipping from 1.0 to 10.0 consistently improved the SuperFedNAS baseline; to ensure rigor, we adopted this stronger setting for both the baseline and DeepFedNAS. We also implement the dynamic weighted averaging scheme from [8], annealing aggregation weights from the largest subnet to a uniform distribution over 80% of the rounds. Total communication rounds are set to 1500 (CIFAR-10), 2000 (CIFAR-100), and 1000 (CINIC-10).

f) Baselines for Comparison: We compare against **FedAvg** [4], **FedNAS** [6], **FedPNAS** [36], and our primary baseline, **SuperFedNAS** [8].

B. Comparison on Image Datasets

We first evaluate DeepFedNAS on three benchmark datasets. As shown in Table II, our method consistently outperforms all baselines across varied computational budgets. The results validate our primary hypothesis: training the supernet on a curriculum of elite, high-fitness architectures yields shared weights that are better conditioned for fine-grained architectural search. On the challenging CIFAR-100 dataset, DeepFedNAS achieves **63.20%** accuracy in the highest MACs bracket, surpassing the tuned SuperFedNAS baseline by nearly a full percentage point and demonstrating a substantial **1.21%** absolute improvement in the 0.95-1.45B MACs range.

C. Impact of Data Heterogeneity

We evaluate robustness against non-IID data by varying the Dirichlet parameter $\alpha \in \{100, 1, 0.1\}$ [50]. As shown in Table III, while all methods degrade with

TABLE III: Comparison across varying degrees of non-IID data on CIFAR-10. DeepFedNAS demonstrates superior robustness, maintaining a significant accuracy advantage, especially in the highly heterogeneous ($\alpha = 0.1$) setting.

Billion MACs	Method	Test Accuracy (%)		
		non-iid-100 ($\alpha = 100$)	non-iid-1 ($\alpha = 1$)	non-iid-0.1 ($\alpha = 0.1$)
0.45-0.95	FedAvg	85.25 \pm 0.46	83.42 \pm 0.19	77.15 \pm 2.5
	FedNAS	77.33 \pm 0.31	71.38 \pm 0.37	61.57 \pm 3.3
	FedPNAS	88.83 \pm 0.5	85.7 \pm 0.4	78.73 \pm 0.45
	SuperFedNAS	93.47 \pm 0.08	91.73 \pm 0.0	85.16 \pm 0.14
0.95-1.45	DeepFedNAS (Ours)	94.16 \pm 0.18	92.84 \pm 0.25	86.01 \pm 0.36
	FedAvg	86.36 \pm 0.22	84.65 \pm 0.11	77.99 \pm 1.6
	FedPNAS	89.27 \pm 0.51	87.53 \pm 0.32	81.13 \pm 0.4
	SuperFedNAS	93.52 \pm 0.17	92.13 \pm 0.12	85.56 \pm 0.18
1.45-2.45	DeepFedNAS (Ours)	94.51 \pm 0.02	93.22 \pm 0.05	86.56 \pm 0.11
	FedAvg	87.59 \pm 0.27	86.14 \pm 0.23	79.93 \pm 1.34
	FedNAS	86.41 \pm 0.1	82.13 \pm 0.65	75.03 \pm 2.57
	SuperFedNAS	93.72 \pm 0.01	92.53 \pm 0.03	85.95 \pm 0.08
2.45-3.75	DeepFedNAS (Ours)	94.50 \pm 0.02	93.29 \pm 0.01	86.80 \pm 0.05
	FedAvg	89.44 \pm 0.67	87.88 \pm 0.7	81.24 \pm 1.99
	FedNAS	89.43 \pm 0.36	85.85 \pm 0.35	68.13 \pm 5.04
	SuperFedNAS	93.72 \pm 0.02	92.63 \pm 0.02	86.00 \pm 0.12
	DeepFedNAS (Ours)	94.51 \pm 0.00	93.33 \pm 0.00	86.83 \pm 0.00

TABLE IV: Comparison across different client participation rates (C) on CIFAR-10. DeepFedNAS maintains its performance lead even with fewer participating clients per round.

Billion MACs	Method	Test Accuracy (%)			
		C = 0.1	C = 0.2	C = 0.4	C = 0.6
0.45-0.95	FedNAS	-	76.23 \pm 0.5	77.33 \pm 0.3	-
	FedPNAS	-	86.63 \pm 0.5	88.83 \pm 0.5	-
	SuperFedNAS	91.52 \pm 0.09	92.41 \pm 0.26	93.47 \pm 0.08	92.99 \pm 0.00
	DeepFedNAS (Ours)	92.98 \pm 0.04	93.59 \pm 0.29	94.16 \pm 0.18	94.13 \pm 0.17
0.95-1.45	FedPNAS	-	87.83 \pm 0.21	89.27 \pm 0.51	-
	SuperFedNAS	92.06 \pm 0.05	92.81 \pm 0.02	93.52 \pm 0.17	93.32 \pm 0.10
	DeepFedNAS (Ours)	93.07 \pm 0.06	94.03 \pm 0.03	94.51 \pm 0.02	94.54 \pm 0.06
	FedNAS	-	84.65 \pm 0.14	86.41 \pm 0.1	-
1.45-2.45	SuperFedNAS	92.35 \pm 0.07	93.01 \pm 0.12	93.72 \pm 0.01	93.93 \pm 0.05
	DeepFedNAS (Ours)	93.30 \pm 0.04	94.05 \pm 0.02	94.50 \pm 0.02	94.79 \pm 0.02
	FedNAS	-	88.0 \pm 0.38	89.43 \pm 0.36	-
	SuperFedNAS	92.31 \pm 0.00	93.04 \pm 0.10	93.72 \pm 0.02	93.94 \pm 0.01
2.45-3.75	DeepFedNAS (Ours)	93.29 \pm 0.00	93.98 \pm 0.00	94.51 \pm 0.00	94.80 \pm 0.00

- Values for FedNAS and FedPNAS were taken from the SuperFedNAS paper and their data at $C=0.1$ and $C=0.6$ was not available for this comparison.

increased heterogeneity (lower α), DeepFedNAS widens its performance lead. In the extreme non-IID setting ($\alpha = 0.1$), our method achieves **86.83%** accuracy in the highest MACs bracket, outperforming the baseline by **0.83%**. This suggests that our Pareto-guided fitness curriculum acts as a regularizer, producing a supernet that is more resilient to the conflicting gradients inherent in heterogeneous data.

D. Impact of Client Participation

We evaluate communication efficiency by varying the client participation rate $C \in \{0.1, 0.2, 0.4, 0.6\}$. Table IV presents results on CIFAR-10. DeepFedNAS demonstrates superior data efficiency, achieving higher accuracy with fewer client updates. For example, in the 0.95-1.45B MACs range, DeepFedNAS with only 10% participation ($C = 0.1$) achieves **93.07%** accuracy. This not only surpasses SuperFedNAS at the same rate (92.06%) but remains competitive with SuperFedNAS at significantly higher participation ($C = 0.4, 93.52\%$). This implies that DeepFedNAS can significantly reduce

communication overhead without compromising model quality.

E. Predictor-Free Search Efficiency

A primary contribution of this work is the elimination of the costly predictor pipeline. We instrumented our framework to measure wall-clock time for each phase (Table V).

The baseline SuperFedNAS approach is burdened by a substantial post-training setup cost: constructing its 10,000-sample predictor dataset requires an exorbitant 20.65 hours on an NVIDIA A5000 GPU. In sharp contrast, DeepFedNAS eliminates this step entirely. After supernet training, our entropy-based fitness function acts as a zero-cost proxy. While DeepFedNAS introduces a pre-training setup (generating the Pareto cache), this process takes only \sim 20 minutes.

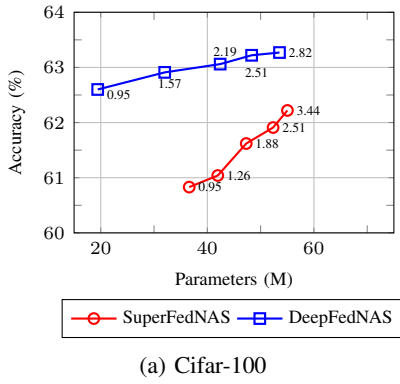
Consequently, DeepFedNAS delivers a substantial **61x speedup** in total pipeline time (auxiliary costs excluding supernet training). An on-demand deployment search completes in a mere \sim 20 seconds, validating that our

unified fitness function eradicates the primary computational bottleneck of existing FedNAS methods.

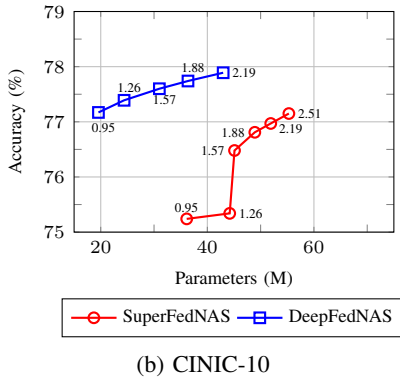
F. Parameter and Communication Efficiency

Efficient federated deployment relies on minimizing model parameters to reduce transmission costs. Figure 3 presents the Pareto frontiers of Test Accuracy vs. Parameters. Figure 3

DeepFedNAS consistently identifies subnets that achieve higher accuracy with significantly fewer parameters. On CIFAR-100, DeepFedNAS achieves $\approx 62.60\%$ accuracy with only 19.43M parameters (0.95B MACs), whereas the baseline requires 55.03M parameters (3.44B MACs) to achieve a lower accuracy of 62.22%. This parameter efficiency directly translates to reduced bandwidth usage and faster aggregation rounds, positioning DeepFedNAS as a superior solution for bandwidth-constrained environments.



(a) Cifar-100



(b) CINIC-10

Fig. 3: **Accuracy vs. Parameters (Millions).** Pareto frontiers for test accuracy percentage against model parameters (Millions) on (a) CIFAR-100 and (b) CINIC-10. DeepFedNAS subnets are blue squares; SuperFedNAS subnets are red circles. Numerical annotations denote MACs in billions.

G. Hardware-Aware Latency Optimization

Neural network design necessitates a trade-off between accuracy and computational efficiency (latency,

MACs). DeepFedNAS addresses this by optimizing subnets via a genetic algorithm guided by device-specific latency prediction models. We empirically validated the discovered architectures on a dedicated Intel Xeon Silver 4210R CPU (@ 2.40 GHz) and an NVIDIA A5000 GPU. Fig. 4 depicts the accuracy-latency Pareto front for CPU deployment, where increased latency correlates with higher accuracy. For example, a subnet achieving 93.67% accuracy (0.62B MACs, ≈ 13.24 ms) contrasts with a higher-capacity model achieving 94.5% accuracy (3.00B MACs, ≈ 31.67 ms). Conversely, inference latency on the A5000 GPU remained consistent (≈ 3.80 – 4.02 ms) across the search space. This divergence in hardware scaling behaviors demonstrates the necessity of the device-specific optimization provided by DeepFedNAS.

Test Accuracy vs True Latency (CPU and GPU)

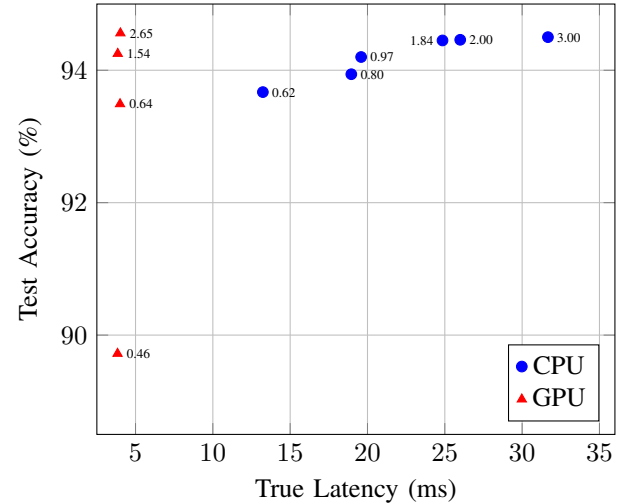


Fig. 4: Test Accuracy vs. True Latency (CPU and GPU). The CPU target is an Intel Xeon Silver 4210R CPU (@ 2.40 GHz), and the GPU target is an NVIDIA RTX A5000. Annotations show subnet MACs in billions.

H. Ablation Studies and Analysis

In this section, we empirically validate the robustness of the DeepFedNAS framework, specifically analyzing the sensitivity of the cache size, the individual contributions of our multi-objective fitness components, and the efficacy of the fitness function as a predictor-free accuracy proxy.

1) *Sensitivity Analysis of Subnet Cache Size:* The size of the optimal path cache, N , determines the granularity of the curriculum used during Federated Supernet Training. To determine the optimal N , we conducted a sensitivity analysis using an equidistant sampling strategy across the computational budget. We measured

TABLE V: Comparison of search costs for a single subnet. DeepFedNAS’s predictor-free approach delivers a dramatic reduction in overall search time.

Search Pipeline Stage	SuperFedNAS (Baseline)	DeepFedNAS (Ours)
Prior to SuperNet Training		
Subnet Cache Generation Time	N/A	~20 minutes (for 60 subnets)
After SuperNet Training		
Predictor Data Generation Time	~20.65 hours	N/A
Predictor Training Time	<i>few minutes</i>	N/A
Search Time per MAC target	~43 seconds	~20 seconds
Total Pipeline Time	~20.65 hours	~20.33 minutes
Speedup Factor	1x	~61x

Baseline’s data generation time is for a 10,000-sample subnet-accuracy dataset.

the population statistics of the generated subnets as N increased from 2 to 200.

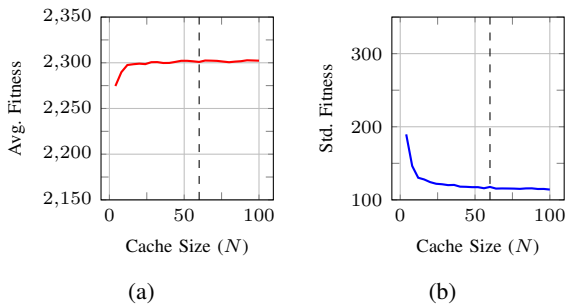


Fig. 5: Analysis of cache size effects: (a) average fitness score and (b) standard deviation of fitness, both vs. cache size ($N = 60$ marked).

As shown in Fig. 5a, we observed a rapid improvement in average architectural fitness, which plateaued in the range of $N = 10\text{--}16$. Concurrently, the standard deviation of fitness scores stabilized in the range of $N = 16\text{--}20$. Consequently, we selected $N = 60$ for all main experiments. This value provides a safety margin that ensures a dense representation of the Pareto frontier and maximizes the diversity of the training curriculum, while remaining computationally efficient.

2) *Component-wise Ablation of Fitness Function*: To validate the individual contributions of the DeepMAD-inspired fitness components defined in Eq. 5, we conducted an ablation study at a constrained computational budget of $\sim 600\text{M}$ MACs on CIFAR-10. We performed independent evolutionary searches ($N = 5$) for each configuration and evaluated the mean test accuracy of the discovered subnets. The results are summarized in Table VI.

a) *Impact of Effectiveness (ρ)*: The baseline approach, maximizing only theoretical entropy (Eq. 6), yields an accuracy of 92.74%. Introducing the effectiveness constraint (ρ) improves performance by 0.43%, confirming that constraining the depth-to-width ratio prevents the selection of degenerate, hard-to-train architectures that theoretically maximize entropy but fail in

TABLE VI: Ablation of Fitness Components ($\sim 600\text{M}$ MACs, CIFAR-10)

Configuration	MACs	Acc. (%)	Gain
1. Entropy Only	599 M	92.74 ± 1.21	-
2. + Effectiveness (ρ)	600 M	93.17 ± 0.77	+0.43%
3. + Depth Pen. (Q)	600 M	93.58 ± 0.33	+0.84%
4. + Chan. Pen. (V)	598 M	93.80 ± 0.16	+1.06%

practice.

b) *Impact of Structural Alignment*: Incorporating structural regularizers yields further significant gains. The Depth Variance Penalty (Q), which encourages balanced stage depths, improves accuracy to 93.58%. Finally, the Non-Decreasing Channel Penalty (V), which enforces standard channel expansion conventions, boosts the final accuracy to **93.80%** (+1.06% over entropy-only based search).

Crucially, Table VI highlights that these structural priors act as powerful regularizers. The inclusion of ρ , Q and V drastically reduces the performance variance from $\pm 1.21\%$ to $\pm 0.16\%$. This stability is vital in federated settings, ensuring that the search consistently discovers optimal architectures regardless of initialization noise.

3) *Validation of Predictor-Free Search Hypothesis*: A central hypothesis of DeepFedNAS is that our constrained supernet training aligns the structural fitness $\mathcal{F}(\mathcal{A})$ with the actual validation accuracy. To validate this, we sampled 60 distinct new architectures evenly distributed along the computational spectrum and evaluated their true validation accuracy against their fitness scores.

The results, presented in Fig. 6, reveal a strong monotonic relationship. We calculated a Spearman rank correlation coefficient of 0.764, confirming a significant positive dependence. This strong correlation substantiates our methodological choice to bypass the training of a latency-heavy accuracy predictor, as maximizing $\mathcal{F}(\mathcal{A})$ is effectively equivalent to maximizing expected accuracy within our supernet regime.

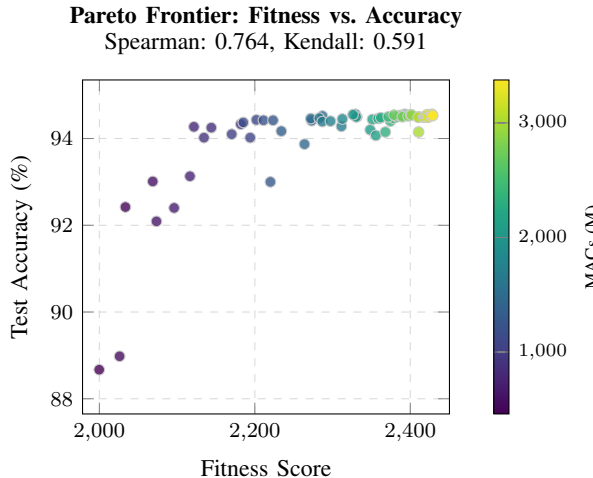


Fig. 6: Correlation analysis validating the predictor-free hypothesis. We observe a strong monotonic relationship (Spearman $\rho = 0.764$) between our fitness score $\mathcal{F}(\mathcal{A})$ and true validation accuracy.

V. LIMITATIONS

While DeepFedNAS demonstrates significant improvements in search efficiency and supernet optimization, we acknowledge certain limitations that open avenues for future research.

First, our experimental evaluation primarily focuses on ResNet-style convolutional search spaces. While these architectures remain the de facto standard for resource-constrained edge deployment due to their hardware friendliness, we have not yet extended our *Pareto-Guided Supernet Training* methodology to Transformer-based architectures (ViTs). Integrating Transformers into a federated supernet introduces distinct challenges regarding stability and communication overhead, which we leave for future work.

Second, our multi-objective fitness function combines information-theoretic concepts with structural regularizers, specifically *depth uniformity* and *channel monotonicity*, to operationalize architectural best practices. While our ablation studies confirm the robustness of these terms across the varied image datasets evaluated (CIFAR-10, CIFAR-100, CINIC-10), adapting the framework to radically different data modalities may benefit from task-specific calibration of these weighting hyperparameters.

Third, consistent with the baseline SuperFedNAS framework [8], our current experimental setup assumes that participating clients possess sufficient computational resources to train the assigned subnets during the supernet training phase. While our framework explicitly solves the problem of constrained *deployment* (inference) by discovering hardware-optimized architectures, we do

not simulate hard hardware constraints (e.g., memory limits preventing backward passes) during the *training* process itself. We identify the integration of system-aware sampling strategies as the immediate next step for DeepFedNAS. By restricting client-subnet assignments based on real-time device capabilities, this extension will bridge the gap towards fully heterogeneous on-device training.

Finally, while our *Predictor-Free Search* dramatically reduces computational costs by using fitness as a zero-shot proxy, it relies on the strong rank correlation established during our path-guided training (Spearman $\rho = 0.764$). While this correlation is robust across the benchmarks evaluated, in theoretical scenarios with extreme noise or insufficient training data, a fully trained surrogate predictor might offer marginally higher ranking precision. DeepFedNAS explicitly prioritizes search efficiency ($61\times$ speedup) over this potential marginal gain.

VI. CONCLUSION

This paper presented DeepFedNAS, a novel framework that fundamentally advances federated neural architecture search by addressing the inefficiencies of unguided supernet training and the prohibitive costs of post-training subnet discovery. Central to DeepFedNAS is a unified, multi-objective fitness function that, combined with a re-engineered supernet, enables two core innovations: Federated Pareto Optimal Supernet Training and a Predictor-Free Search Method. The former leverages a pre-computed “Pareto path” of elite architectures as an intelligent curriculum for supernet weight optimization, yielding robust models. The latter capitalizes on this well-conditioned supernet, allowing our fitness function to serve as a direct, zero-cost proxy for subnet accuracy, enabling on-demand architectural searches in just 20 seconds. DeepFedNAS consistently achieved state-of-the-art accuracy, demonstrated superior parameter and communication efficiency, and crucially, delivered a substantial $\sim 61\times$ speedup in total post-training search pipeline time (reducing from over 20 hours to 20 minutes, including initial cache generation). These results position DeepFedNAS as a highly efficient, accurate, and adaptable solution for deploying optimal neural networks in diverse and resource-constrained federated environments, marking a significant step towards truly practical and scalable FedNAS.

REFERENCES

- [1] B. Khan and M. Daneshbalab, “Deepfednas: Pareto optimal supernet training for improved and predictor-free federated neural architecture search,” in *34th European Symposium on Artificial Neural Networks, Computational Intelligence and Machine Learning*, 2026. [Online]. Available: <http://www.es.mdu.se/publications/7335>

- [2] A. Hard, K. Rao, R. Mathews, F. Beaufays, S. Augenstein, H. Eichner, C. Kiddon, and D. Ramage, “Federated learning for mobile keyboard prediction,” *CoRR*, vol. abs/1811.03604, 2018. [Online]. Available: <http://arxiv.org/abs/1811.03604>
- [3] S. Silva, B. A. Gutman, E. Romero, P. M. Thompson, A. Altmann, and M. Lorenzi, “Federated learning in distributed medical databases: Meta-analysis of large-scale subcortical brain data,” in *2019 IEEE 16th International Symposium on Biomedical Imaging (ISBI 2019)*, 2019, pp. 270–274.
- [4] B. McMahan, E. Moore, D. Ramage, S. Hampson, and B. A. y. Arcas, “Communication-Efficient Learning of Deep Networks from Decentralized Data,” in *Proceedings of the 20th International Conference on Artificial Intelligence and Statistics*, ser. Proceedings of Machine Learning Research, A. Singh and J. Zhu, Eds., vol. 54. PMLR, 20–22 Apr 2017, pp. 1273–1282.
- [5] T. Li, A. K. Sahu, M. Zaheer, M. Sanjabi, A. Talwalkar, and V. Smith, “Federated optimization in heterogeneous networks,” in *Proceedings of Machine Learning and Systems*, I. Dhillon, D. Papailiopoulos, and V. Sze, Eds., vol. 2, 2020, pp. 429–450.
- [6] C. He, M. Annavaram, and S. Avestimehr, “FedNAS: Federated deep learning via neural architecture search,” *CoRR*, vol. abs/2004.08546, 2020. [Online]. Available: <https://arxiv.org/abs/2004.08546>
- [7] H. Cai, C. Gan, and S. Han, “Once-for-All: Train one network and specialize it for efficient deployment,” *CoRR*, vol. abs/1908.09791, 2019. [Online]. Available: <http://arxiv.org/abs/1908.09791>
- [8] A. Khare, A. Agrawal, A. Annavajjala, P. Behnam, M. Lee, H. Latapie, and A. Tumanov, “SuperFedNAS: Cost-efficient federated neural architecture search for on-device inference,” in *Computer Vision – ECCV 2024*, A. Leonardis, E. Ricci, S. Roth, O. Russakovsky, T. Sattler, and G. Varol, Eds. Cham: Springer Nature Switzerland, 2024, pp. 161–179.
- [9] J. Yu and T. S. Huang, “Universally slimmable networks and improved training techniques,” in *Proceedings of the IEEE/CVF International Conference on Computer Vision (ICCV)*, October 2019.
- [10] X. Shen, Y. Wang, M. Lin, Y. Huang, H. Tang, X. Sun, and Y. Wang, “DeepMAD: Mathematical architecture design for deep convolutional neural network,” in *Proceedings of the IEEE/CVF Conference on Computer Vision and Pattern Recognition (CVPR)*, June 2023, pp. 6163–6173.
- [11] K. He, X. Zhang, S. Ren, and J. Sun, “Deep residual learning for image recognition,” *CoRR*, vol. abs/1512.03385, 2015. [Online]. Available: <http://arxiv.org/abs/1512.03385>
- [12] B. Liu, N. Lv, Y. Guo, and Y. Li, “Recent advances on federated learning: A systematic survey,” *Neurocomputing*, vol. 597, p. 128019, 2024. [Online]. Available: <https://www.sciencedirect.com/science/article/pii/S0925231224007902>
- [13] P. Kairouz, H. B. McMahan, B. Avent, A. Bellet, M. Bennis, A. N. Bhagoji, K. Bonawitz, Z. Charles, G. Cormode, R. Cummings, R. G. L. D’Oliveira, H. Eichner, S. E. Rouayheb, D. Evans, J. Gardner, Z. Garrett, A. Gascón, B. Ghazi, P. B. Gibbons, M. Gruteser, Z. Harchaoui, C. He, L. He, Z. Huo, B. Hutchinson, J. Hsu, M. Jaggi, T. Javidi, G. Joshi, M. Khodak, J. Konecný, A. Korolova, F. Koushanfar, S. Koyejo, T. Lepoint, Y. Liu, P. Mittal, M. Mohri, R. Nock, A. Özgür, R. Pagh, H. Qi, D. Ramage, R. Raskar, M. Raykova, D. Song, W. Song, S. U. Stich, Z. Sun, A. T. Suresh, F. Tramèr, P. Vepakomma, J. Wang, L. Xiong, Z. Xu, Q. Yang, F. X. Yu, H. Yu, and S. Zhao, “Advances and open problems in federated learning,” *Foundations and Trends® in Machine Learning*, vol. 14, no. 1–2, pp. 1–210, 2021. [Online]. Available: <http://dx.doi.org/10.1561/2200000083>
- [14] T. Li, A. K. Sahu, A. Talwalkar, and V. Smith, “Federated learning: Challenges, methods, and future directions,” *IEEE Signal Processing Magazine*, vol. 37, no. 3, pp. 50–60, 2020.
- [15] L. Cooray, J. Sendanayake, P. Vithanaarachchi, and Y. H. P. P. Priyadarshana, “Deep federated learning: a systematic review of methods, applications, and challenges,” *Frontiers in Computer Science*, vol. Volume 7 - 2025, 2025. [Online]. Available: <https://www.frontiersin.org/journals/computer-science/articles/10.3389/fcomp.2025.1617597>
- [16] J. Konečný, H. B. McMahan, F. X. Yu, P. Richtárik, A. T. Suresh, and D. Bacon, “Federated learning: Strategies for improving communication efficiency,” *CoRR*, vol. abs/1610.05492, 2016. [Online]. Available: <http://arxiv.org/abs/1610.05492>
- [17] Z. Lu, H. Pan, Y. Dai, X. Si, and Y. Zhang, “Federated learning with non-iid data: A survey,” *IEEE Internet of Things Journal*, vol. 11, no. 11, pp. 19 188–19 209, 2024.
- [18] D. Makhija, J. Ghosh, and N. Ho, “A bayesian approach for personalized federated learning in heterogeneous settings,” in *Advances in Neural Information Processing Systems*, A. Globerson, L. Mackey, D. Belgrave, A. Fan, U. Paquet, J. Tomczak, and C. Zhang, Eds., vol. 37. Curran Associates, Inc., 2024, pp. 102 428–102 455.
- [19] Y. Tan, G. Long, L. Liu, T. Zhou, Q. Lu, J. Jiang, and C. Zhang, “Fedproto: Federated prototype learning across heterogeneous clients,” 2022. [Online]. Available: <https://arxiv.org/abs/2105.00243>
- [20] A.-J. Farcas, X. Chen, Z. Wang, and R. Marculescu, “Model elasticity for hardware heterogeneity in federated learning systems,” in *Proceedings of the 1st ACM Workshop on Data Privacy and Federated Learning Technologies for Mobile Edge Network*, ser. FedEdge ’22. New York, NY, USA: Association for Computing Machinery, 2022, p. 19–24. [Online]. Available: <https://doi.org/10.1145/3556557.3557954>
- [21] B. Zoph and Q. V. Le, “Neural architecture search with reinforcement learning,” *CoRR*, vol. abs/1611.01578, 2016. [Online]. Available: <http://arxiv.org/abs/1611.01578>
- [22] C. Liu, B. Zoph, M. Neumann, J. Shlens, W. Hua, L.-J. Li, L. Fei-Fei, A. Yuille, J. Huang, and K. Murphy, “Progressive neural architecture search,” in *Proceedings of the European Conference on Computer Vision (ECCV)*, September 2018.
- [23] G. Bender, P.-J. Kindermans, B. Zoph, V. Vasudevan, and Q. Le, “Understanding and simplifying one-shot architecture search,” in *Proceedings of the 35th International Conference on Machine Learning*, ser. Proceedings of Machine Learning Research, J. Dy and A. Krause, Eds., vol. 80. PMLR, 10–15 Jul 2018, pp. 550–559.
- [24] L. Xie, X. Chen, K. Bi, L. Wei, Y. Xu, L. Wang, Z. Chen, A. Xiao, J. Chang, X. Zhang, and Q. Tian, “Weight-sharing neural architecture search: A battle to shrink the optimization gap,” *ACM Comput. Surv.*, vol. 54, no. 9, Oct. 2021.
- [25] H. Liu, K. Simonyan, and Y. Yang, “DARTS: Differentiable architecture search,” in *International Conference on Learning Representations*, 2019. [Online]. Available: <https://openreview.net/forum?id=S1eYHoCSFX>
- [26] J. Yu, P. Jin, H. Liu, G. Bender, P.-J. Kindermans, M. Tan, T. Huang, X. Song, R. Pang, and Q. Le, “Bignas: Scaling up neural architecture search with big single-stage models,” in *Computer Vision – ECCV 2020*, A. Vedaldi, H. Bischof, T. Brox, and J.-M. Frahm, Eds. Cham: Springer International Publishing, 2020, pp. 702–717.
- [27] J. Pan, C. Sun, Y. Zhou, Y. Zhang, and C. Li, “Distribution consistent neural architecture search,” in *2022 IEEE/CVF Conference on Computer Vision and Pattern Recognition (CVPR)*, 2022, pp. 10 874–10 883.
- [28] M. Zhang, H. Li, S. Pan, X. Chang, and S. Su, “Overcoming multi-model forgetting in one-shot nas with diversity maximization,” in *2020 IEEE/CVF Conference on Computer Vision and Pattern Recognition (CVPR)*, 2020, pp. 7806–7815.
- [29] L. Ma, Y. Zhou, Y. Ma, G. Yu, Q. Li, Q. He, and Y. Pei, “Defying multi-model forgetting in one-shot neural architecture search using orthogonal gradient learning,” *IEEE Transactions on Computers*, vol. 74, no. 5, pp. 1678–1689, 2025.
- [30] Y. Venkatesha, Y. Kim, H. Park, and P. Panda, “Divide-and-conquer the nas puzzle in resource-constrained federated learning systems,” *Neural Networks*, vol. 168, pp. 569–579, 2023. [Online]. Available: <https://www.sciencedirect.com/science/article/pii/S0893608023005609>

- [31] H. Wang, C. Ge, H. Chen, and X. Sun, "PreNAS: Preferred one-shot learning towards efficient neural architecture search," in *Proceedings of the 40th International Conference on Machine Learning*, ser. Proceedings of Machine Learning Research, A. Krause, E. Brunskill, K. Cho, B. Engelhardt, S. Sabato, and J. Scarlett, Eds., vol. 202. PMLR, 23–29 Jul 2023, pp. 35 642–35 654. [Online]. Available: <https://proceedings.mlr.press/v202/wang23f.html>
- [32] A. Garg, A. K. Saha, and D. Dutta, "Direct federated neural architecture search," 2020. [Online]. Available: <https://arxiv.org/abs/2010.06223>
- [33] J. Yuan, M. Xu, Y. Zhao, K. Bian, G. Huang, X. Liu, and S. Wang, "Resource-aware federated neural architecture search over heterogeneous mobile devices," *IEEE Transactions on Big Data*, pp. 1–11, 2022.
- [34] H. R. Roth, D. Yang, W. Li, A. Myronenko, W. Zhu, Z. Xu, X. Wang, and D. Xu, "Federated whole prostate segmentation in mri with personalized neural architectures," in *Medical Image Computing and Computer Assisted Intervention – MICCAI 2021*, M. de Bruijne, P. C. Cattin, S. Cotin, N. Padov, S. Speidel, Y. Zheng, and C. Essert, Eds. Cham: Springer International Publishing, 2021, pp. 357–366.
- [35] J. Yan, J. Liu, H. Xu, Z. Wang, and C. Qiao, "Peaches: Personalized federated learning with neural architecture search in edge computing," *IEEE Transactions on Mobile Computing*, vol. 23, no. 11, pp. 10 296–10 312, 2024.
- [36] M. Hoang and C. Kingsford, "Personalized neural architecture search for federated learning," *1st NeurIPS Workshop on New Frontiers in Federated Learning (NFFL 2021)*, 2021.
- [37] D. Yao, L. Wang, J. Xu, L. Xiang, S. Shao, Y. Chen, and Y. Tong, "Federated model search via reinforcement learning," in *2021 IEEE 41st International Conference on Distributed Computing Systems (ICDCS)*, 2021, pp. 830–840.
- [38] D. Yao and B. Li, "Perfedrnas: One-for-all personalized federated neural architecture search," *Proceedings of the AAAI Conference on Artificial Intelligence*, vol. 38, no. 15, pp. 16 398–16 406, Mar. 2024. [Online]. Available: <https://ojs.aaai.org/index.php/AAAI/article/view/29576>
- [39] Y. Liu, S. Guo, J. Zhang, Z. Hong, Y. Zhan, and Q. Zhou, "Collaborative neural architecture search for personalized federated learning," *IEEE Transactions on Computers*, vol. 74, no. 1, pp. 250–262, 2025.
- [40] A. Yang and Y. Liu, "Heterogeneity-aware personalized federated neural architecture search," *Entropy*, vol. 27, no. 7, 2025. [Online]. Available: <https://www.mdpi.com/1099-4300/27/7/759>
- [41] S. Horvath, S. Laskaridis, M. Almeida, I. Leontiadis, S. Venieris, and N. Lane, "Fjord: Fair and accurate federated learning under heterogeneous targets with ordered dropout," *Advances in Neural Information Processing Systems*, vol. 34, pp. 12 876–12 889, 2021.
- [42] X. Wang, Y. Zhao, C. Qiu, F. Gao, Z. Zhao, H. Yao, and X. Li, "Energy-friendly federated neural architecture search for industrial cyber-physical systems," *IEEE Journal on Selected Areas in Communications*, vol. 43, no. 10, pp. 3502–3518, 2025.
- [43] J. Liu, J. Yan, H. Xu, Z. Wang, J. Huang, and Y. Xu, "Finch: Enhancing federated learning with hierarchical neural architecture search," *IEEE Transactions on Mobile Computing*, vol. 23, no. 5, pp. 6012–6026, 2024.
- [44] J. Yuan, M. Xu, Y. Zhao, K. Bian, G. Huang, X. Liu, and S. Wang, "Resource-aware federated neural architecture search over heterogeneous mobile devices," *IEEE Transactions on Big Data*, pp. 1–11, 2022.
- [45] E. Real, A. Aggarwal, Y. Huang, and Q. V. Le, "Regularized evolution for image classifier architecture search," *Proceedings of the AAAI Conference on Artificial Intelligence*, vol. 33, no. 01, pp. 4780–4789, Jul. 2019. [Online]. Available: <https://ojs.aaai.org/index.php/AAAI/article/view/4405>
- [46] H. Fang, Y. Gao, P. Zhang, J. Yao, H. Chen, and H. Wang, "Large language models enhanced personalized graph neural architecture search in federated learning," *Proceedings of the AAAI Conference on Artificial Intelligence*, vol. 39, no. 16, pp. 16 514–16 522, Apr. 2025. [Online]. Available: <https://ojs.aaai.org/index.php/AAAI/article/view/33814>
- [47] R. Qin, Y. Hu, Z. Yan, J. Xiong, A. Abbasi, and Y. Shi, "Fl-nas: Towards fairness of nas for resource constrained devices via large language models," in *Proceedings of the 29th Asia and South Pacific Design Automation Conference*, ser. ASPDAC '24. IEEE Press, 2024, p. 429–434. [Online]. Available: <https://doi.org/10.1109/ASP-DAC58780.2024.10473847>
- [48] S. Namekawa and T. Tezuka, "Evolutionary neural architecture search by mutual information analysis," in *2021 IEEE Congress on Evolutionary Computation (CEC)*, 2021, pp. 966–972.
- [49] L. Gao, H. Fu, L. Li, Y. Chen, M. Xu, and C.-Z. Xu, "Feddc: Federated learning with non-iid data via local drift decoupling and correction," in *Proceedings of the IEEE/CVF Conference on Computer Vision and Pattern Recognition (CVPR)*, June 2022, pp. 10 112–10 121.
- [50] T.-M. H. Hsu, H. Qi, and M. Brown, "Measuring the effects of non-identical data distribution for federated visual classification," 2019. [Online]. Available: <https://arxiv.org/abs/1909.06335>